

# Grid-Aware Waveform Analytics for Event Classification in Distribution Grids

Mohammad MansourLakouraj<sup>1</sup>, *Student Member, IEEE*, Hadis Hosseinpour<sup>2</sup>, *Student Member, IEEE*, Hanif Livani<sup>1</sup>, *Senior Member, IEEE*, and Mohammed Benidris<sup>2</sup>, *Senior Member, IEEE*

<sup>1</sup>Department of Electrical & Biomedical Engineering, University of Nevada, Reno, Reno, NV

<sup>2</sup>Department of Electrical and Computer Engineering, Michigan State University, East Lansing, MI 48824

Emails: mansour@nevada.unr.edu, hossei13@msu.edu, hlivani@unr.edu and benidris@msu.edu

**Abstract**—This study proposes a new method for event situational awareness in distribution grids using Synchro Waveform Measurement Units (SWMUs). An efficient feature-extracting technique named the Short-Time Matrix Pencil method (STMPM) is used to capture the oscillation modes and distortion of voltage and current measurements under common events such as transient switching events and challenging high impedance faults. The extracted features from the waveform data are then used as the input to Graph Neural Network (GNN) as the event classifier. GNN captures the spatial relationship between SWMUs and physical features of the network to enhance event classification accuracy. The proposed grid-aware waveform analytics is tested for classifying different events, and the superior performance of the proposed method with respect to other approaches is verified using the classification merits, such as accuracy, F1-score, precision, and recall.

**Index Terms**—Distribution Grids, Event Classification, Graph Neural Network, Waveform Measurement, Matrix Pencil Method.

## I. INTRODUCTION

Different types of disturbances and outages can occur in distribution systems, which require better situational awareness to improve system recovery and enhance grid reliability and resilience [1], [2]. Switching *transient* events and high impedance faults (HIF) are among the most widespread events in distribution systems. Transient events cause instantaneous distortion in voltage or current signals, which can be captured using sensors with high sampling rates. Moreover, HIFs usually create small and insignificant variations in current or voltage signals, making them much harder to detect using conventional protection devices, such as overcurrent protection with predetermined sensitivity thresholds [3]. HIFs may cause stochastic arcing behavior that can initiate wildfires and become safety hazards. Thus, developing an efficient event classification method and having access to high-sampling-rate measurement can assist system operators and protection engineers in performing suitable corrective, remedial, preventive, or maintenance actions corresponding to the detected event.

The evolution of advanced sensors and measurement devices has begun with the vast deployment of phasor measurement units (PMUs) for grid situational awareness. The sampling rate of PMUs usually varies between 30 to 120 samples-per-second (SPS) [4]. However, PMUs may not capture enough information for transient event analysis. For transient events, such as HIFs and switching events, current or voltage dis-

tortions can be better captured using higher sampling rate waveform sensors. Therefore, there have been recent interests in exploring the use of high sampling rate measurements, named synchro waveform measurement units (SWMUs) for different applications, including events analysis [5]. The reporting rate of SWMUs can go up to 256 sample-per-cycle, which help to detect and identify transient event with *minor* signal distortions.

Event classification methods are broadly categorized into data-driven-based, model-based, and grid-informed data-driven models. Under the data-driven-based category, in [4], a PMU-based classification method is proposed using an autoencoder to classify different events. In a recent study, a CNN-based classifier and short-time Fourier transform (STFT) are proposed to identify the cause of faults using waveform data [6]. In [7], the Hierarchical Bayesian Program Learning (HBPL) is adopted to classify the incipient faults versus capacitor bank (CB) switching and load changes using the human-level concept for extracting features of waveform measurements. In [8], the Prony modal analysis of synchro waveform data is conducted, and the circuit model is built using the obtained modes to locate transient events and faults. However, model-based techniques require accurate modeling of the circuit with various components which adds to the complexity of the proposed method. In this paper, we overcome the existing gaps between data-drive and purely circuit-based approaches by using a grid-aware data-driven classifier, named Graph Neural Network (GNN) combined with short-time modal analysis, named Short-Time Matrix Pencil Method (STMPM) for signals feature extraction [9]. In [10], GNN is adopted for locating faults using phasor measurement data in active distribution systems. Authors of [11] uses GNN for event classification in active distribution networks. In [12], GNN is implemented for event classification and region identification in active distribution grids with multi-sampling rate PMUs and GNN's edge features. Authors of [13] propose GNN-based event clustering with fundamental and harmonic PMU data in conventional distribution feeders without considering edge features in GNN. The GNN is used with waveform signals and short-time modal analysis under regular faults, while challenging events such as arc-based HIF and transient switching events are not studied [14]. With respect to the stated research gaps, the contributions of this

paper are as follows:

- This paper investigates the challenging problem of event classification in distribution systems with a new emerging class of high-sampling rate measurements, called SWMUs, to enhance network situational awareness.
- Short-time matrix pencil method (STMPM) is proposed to extract waveforms' features and signatures for transient and permanent events classification.
- The spatial relationship of the locationally-scarce SWMUs and the grid topological features are incorporated in the GNN model as a *grid-aware* event classifier.

The rest of the paper is organized as follows. The GNN and STMPM are explained in Sections II and III. Moreover, Section IV discusses different case studies and data preparation. Section V presents the numerical studies, and VI concludes the studies.

## II. GRAPH NEURAL NETWORK

A distribution network is defined as an undirected graph  $G = (V, E, A)$ , where  $V$ ,  $E$ , and  $A$  show the set of nodes, set of edges, and adjacency matrix of the graph, respectively. The matrix  $A$  implies the topological feature, where its greater elements are showing a stronger correlation between particular nodes. Considering the nodal correlations of power grids, a distance-based metric is defined as  $l_{ij} = 1/m_{ij}$ , indicating an element of  $A$ . Here,  $m_{ij}$  shows the physical distance between two nodes [12]. Moreover, matrix  $D$  represents the number of nodes connected to that particular node. The spectral convolution in the Fourier domain is given as the multiplication of signal  $z$ , including nodal voltages and currents, with a parameterized filter  $\psi_\theta$ . A re-normalization technique is used [15], resulting in modified convolution as (1), where  $\hat{A} = I + A$ , and  $\hat{D}_{ii} = \sum_j \hat{A}_{ij}$  are defined.

$$\psi_\theta * z = \theta(\hat{D}^{-0.5} \hat{A} \hat{D}^{-0.5}) z \quad (1)$$

Equation (1) is extended to (2), where matrix  $Z \in R^{N \times M}$  considered instead of  $z$  which has a scalar for each node. The data stream has  $M$  features recorded by SWMUs before and after occurring the event. The matrix  $B \in R^{M \times Q}$  represents the parameter of filters with  $Q$  feature maps. Finally, graph convoluted signals are given in matrix  $H$ . This definition is used to design the GNN framework with multi Graph Convolution layers followed by the linear transformer and softmax classifier. An activation function (ReLU) is used between graph convolution layers [12].

$$H = (\hat{D}^{-0.5} \hat{A} \hat{D}^{-0.5}) Z B \quad (2)$$

## III. FEATURE ENGINEERING WITH STMPM

A band-limited signal defined in a period of  $T$  is represented by an extended form of Fourier series, as (3). In (3), damping factor is indicated as  $-\alpha_i$  in  $sec^{-1}$ , and the angular speed is specified with  $\omega_i$  in  $rad.sec^{-1}$ , giving the complex frequency. Moreover,  $r_i$  is the residual of the signal. Note that if  $\alpha_i$  is equated with 0, Equation (3) will be represented as Fourier

series. However,  $\alpha_i$  contains very informative details of the system, motivating us to use this generic formulation [16].

$$Z(t) = \sum_{i=1}^N r_i e^{-\alpha_i t} \cos(\omega_i t + \theta_i) \quad (3)$$

Considering this definition, we can reconstruct the observed signal in a specified length of the window using STMPM and use its driven signal components ( $\alpha_i$ ,  $\omega_i$  and  $r_i$ ) as selected features from raw signal for event cause analysis. In our analysis,  $Z(t)$  is defined as *alpha* elements of Clark transformation for three-phase voltages monitored by an SWMU. This indicates the real part of space vectors, shrinking the data dimension and capturing distortion in all three-phase voltage signals. The mathematical definition of STMPM is elaborated on in this section. The matrix  $W$  shown in (4) is made by captured samples in an  $N$ -sample sliding window.

$$W = \begin{bmatrix} Z(1) & Z(2) & \dots & Z(P+1) \\ Z(2) & Z(3) & \dots & Z(P+2) \\ \vdots & \vdots & \vdots & \vdots \\ Z(N-P) & Z(N-P+1) & \dots & Z(N) \end{bmatrix} \quad (4)$$

where  $Z(\cdot)$  and  $N$  imply the original sample and sample numbers in the sliding window, respectively. Moreover,  $P$  is a matrix pencil parameter defined between  $N/3$  to  $N/2$  [17], adjusted for filtering the noise. The dimension of matrix  $W$  is  $(N - P) \times (P + 1)$ . The singular-value decomposition (SVD) of  $W$  is done as follows:

$$Y = WW^H, \quad V = W^H W \quad (5)$$

$$W = U_Y \sum U_V^H \quad (6)$$

where  $(\cdot)^H$  and  $U_{(\cdot)}$  indicate complex conjugate and unitary matrix with eigenvectors, respectively.  $\sum$  constructed by singular values of  $W$  indicates a diagonal matrix. Also, a threshold is confined as (7) to choose the singular dominant values. In (7),  $f$  is the filtering factor, and the dominant and maximum singular value are as  $\eta_d$  and  $\eta_m$ , respectively [17].

$$\eta_m 10^{-f} \leq \eta_d \quad (7)$$

The columns of the matrix  $\sum$  that correspond to the dominant singular values are retained, and the remaining columns are discarded. Consequently,  $\sum'$  defines the reduced matrix. Additionally, the matrix  $U_V$  is modified as  $U_V'$  by preserving only its columns that are associated with the dominant singular values, while discarding the remaining columns.  $W_{first}$  and  $W_{last}$  are defined in (8).

$$W_{first} = U_Y \sum' U_{V,first}^H, \quad W_{last} = U_Y \sum' U_{V,last}^H \quad (8)$$

where  $U_{V,first}'$  is obtained by excluding the last row of  $U_V'$  and  $U_{V,last}'$  is obtained by omitting the first row in  $U_V'$ . Finally, the following formulas are presented:

$$|W_{first}^+ W_{last} - \lambda I| = 0 \quad (9)$$

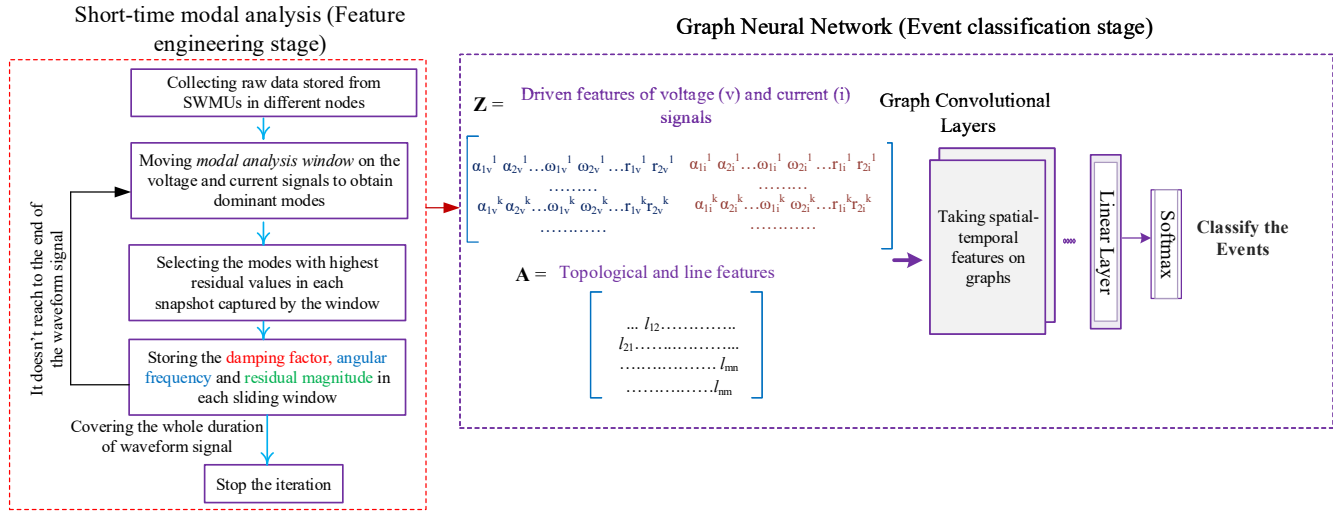


Fig. 1. Schematic of the grid-aware waveform analytics for event classification

In (9),  $\lambda$  denotes eigen root of (9) and Moore–Penrose pseudoinverse is shown  $(.)^+$ . The relationship between eigenvalues and complex frequencies is as (10) [17].

$$\lambda_n = e^{(-\alpha_n \pm j\omega_n)T_{sp}}, \quad \forall n = 1, 2, \dots, m \quad (10)$$

where  $T_{sp}$  and  $\lambda_n$  are the sampling period and eigenvalues. By driving the eigenvalues, complex frequencies are obtained in each snapshot, shown in (11).

$$-\alpha_n \pm j\omega_n = \ln(\lambda_n)/T_{sp}, \quad \forall n = 1, 2, \dots, m \quad (11)$$

The process proposed in (4)–(11) for each snapshot is repeated until the sliding window arrives to the end of the signal, guaranteeing a short-time modal analysis.

#### A. Short-time feature selection for event classification

STMPM is applied on waveform data to characterize oscillatory modes included in distribution system responses against an event. Characteristics of modes are different in each event, enabling us to identify events type. A set of features including damping factors, angular frequencies, and residual magnitude related to the dominant mode are obtained from each sliding window. To capture these informative features (event signatures), several steps are defined to make a new set for voltage and current signals as follows: (1) Extracting the dominant modes and corresponding residues of the waveform data in each sliding window. This is possible by creating matrix  $X$  and applying SVD on it as explained in Section III. (2) Choosing the mode that has the highest corresponding residual value in each snapshot compared to the obtained modes. Depending on the event type, the number of modes is more or less. For example, CB switching makes significant oscillation, creating new modes. HIF does not create observable distortion, and it usually has two fundamental modes with small variations. (3) Saving the damping factor, angular frequency, and residual obtained from voltage and current signals, recorded in

each snapshot. Vectors are created for voltage and current features separately. (4) Keep storing three distinctive pieces of information until the sliding window passes the event monitoring interval. (5) Combining the captured features of voltage and current vectors as the signature of events driven from a particular sensor. This process is performed for each sensor, and their relevant information is transferred to the measurement matrix ( $Z$ ). Fig. 1 shows the process of feature extraction and the GNN-based classification in the grid-aware waveform analytics.

#### IV. CASE STUDY AND DATA PREPARATION

The proposed model is tested on the modified IEEE 13-bus system, as illustrated in Fig. 2. The node numbers defined in the IEEE system are changed to contain 0-12 node numbers for the GNN adjacency matrix. A non-dispatchable Distributed energy resource (DER) with a base capacity of 1 MW is added to node 6. The base consumption of three-phase and single-phase loads are 1 MW per phase and 0.12 MW on nodes 3 and 12, respectively. The permanent outage of DER and the transient disconnection of loads with the duration of 1 and 2 cycles are considered as individual events in this study. Additionally, a three-phase capacitor bank (CB) installed on node 8 can provide 75 kVar power per phase, and a single-phase CB installed on node 11 provides 45.98 kVar reactive power. These CBs can experience transient switching and permanent disconnection from the system. Arc-based HIF faults occur on nodes 2, 4, or 8, and their stochastic behavior is modeled by the diode-based circuit and the parameters adopted from [18]. The impedance of these faults changes between 100-150 ohms during the simulation period, ensuring the uncertainty in the type of contacted surface and the arc variations. It is considered that a single-phase HIF can occur since this is the most common type of HIF event. Regular symmetric and asymmetric low-impedance faults occur on

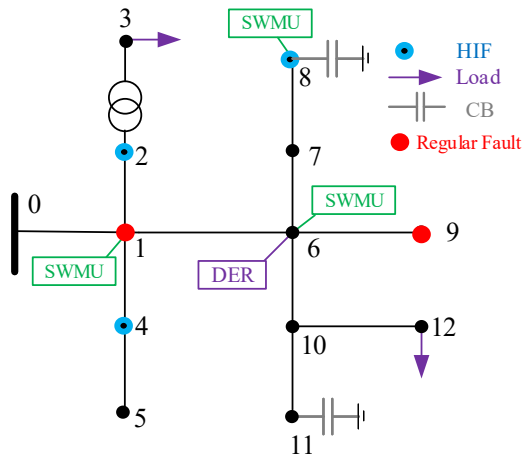


Fig. 2. The schematic of the modified IEEE 13-bus grid

nodes 1 and 9 with a transient duration of 1 and 2 cycles. The resistance of such faults is between 0.01 and 1 ohm. Moreover, three SWMUs with a sampling rate of 256 samples per cycle are assumed to be installed on nodes 1, 6, and 8. The PSCAD software automated through its Python API is used to generate a database of these realistic events under probable real-world conditions, such as system loading and DER generations. The grid conditions are considered by changing DER output between 100 kW to 1300 kW and modifying loads between 80% to 130% of the base consumption of nodes. The waveform data are modified by adding Gaussian noise with different signal-to-noise rates (SNR) of 45, 50, 55, 60 dBs to the raw data. Also, 9 equally divided inception points are considered on a cycle to consider different events' inception angles. Finally, six different labels corresponding to different event types and the normal condition are considered, as indicated in Table I. It is to be noted that we assumed that voltage and current waveforms with high sampling rates are available on only three nodes because of the locationally scarcity of SWMUs. Note that the main cost is related to storing the data, which is reducing by the improvement of storage technologies [5]. To train the GNN model, more than 6000 sample events are prepared.

#### A. Parameters of GNN and STMPM

The GNN architecture is set with two GCN layers, each with 128 channels, followed by a linear transformation including 256 hidden nodes. ReLu is the activation function between GCN layers, and the dropout rate is set at 0.5. Adam optimizer is considered with a learning rate of 0.0001, and the batch size is 8. Softmax classifier is also located as the last layer for event classification with the cross entropy as the loss function of the classifier. As for the STMPM, the length of the sliding window is equal to 9.1 ms, and the step size of the moving window is 2.6 ms. The parameter  $f$  is 3 [14], [16]. These parameters are optimally adjusted based on several rounds of experiments.

TABLE I  
EVENTS AND LABELS

| Labels | Event Type (Duration of the event)                   |
|--------|--|
| 0      | CB's switching malfunction (Transient and permanent) |
| 1      | DER outage (Permanent)                               |
| 2      | Load disconnection (Transient)                       |
| 3      | Arc-based HIFs (Transient and permanent)             |
| 4      | Regular faults (Transient)                           |
| 5      | Normal condition                                     |

## V. NUMERICAL ANALYSIS

In this section, the captured features from waveform data and the event classification performance are studied. Several metrics such as macro-average F1 score, recall, and precision are used for evaluating the classification performance [12].

TABLE II  
THE RESULTS COMPARISON

| Different Approaches | Average Accuracy % | Best Accuracy % | Macro Pre % | Macro F1 % | Macro Rec % |
|----------------------|--------------------|-----------------|-------------|------------|-------------|
| <i>GNN</i>           | 98.53              | 99.08           | 98.34       | 97.92      | 97.55       |
| <i>DT</i>            | 95.04              | 95.79           | 94.22       | 94.01      | 93.84       |
| <i>kNN</i>           | 90.29              | 90.90           | 90.48       | 90.49      | 94.69       |

### A. Extracted features

Illustrative examples given in Fig. 3 show the extracted features using STMPM from the voltage signals for CB switching and HIF events. The voltage is obtained from the alpha component of three-phase voltages transformed through a Clark transformation. Fig. 3.a indicates that a transient CB switching on node 8 causes oscillations on the voltage and makes new transient oscillatory modes in the system, which are captured by the SWMU at the same location, with SNR of 45 dB. Three informative features named dominant damping factor, angular frequency, and residual magnitude detect the instantaneous changes caused by the event, as illustrated on the right-hand side of the raw waveform signal. For a 60-Hz system, the base angular frequency is  $377 \approx 2\pi 60$  rad/sec, and it raises to 419.54 rad/sec during the switching event. The stream of the captured features is obtained by moving the sliding window along the waveform data and mapping the dominant mode features in each snapshot to the shown streamed features. Each stream of features is now represented by 32 points, leading to 96 samples overall for the three selected features, representing the dynamic response of the grid under a particular event. As another example, a HIF occurs on node 2, and the SWMU located on node 1 records the three-phase voltages which are then transformed using the Clark transformation shown in Fig. 3.b. Since the signal distortion caused by this HIF with a variable resistor is hard to detect, the zoomed version of the alpha mode voltage is also shown. As can be seen, the amount of changes in the waveform signal is very small and hard to detect. However, the three extracted features by the STMPM can capture some

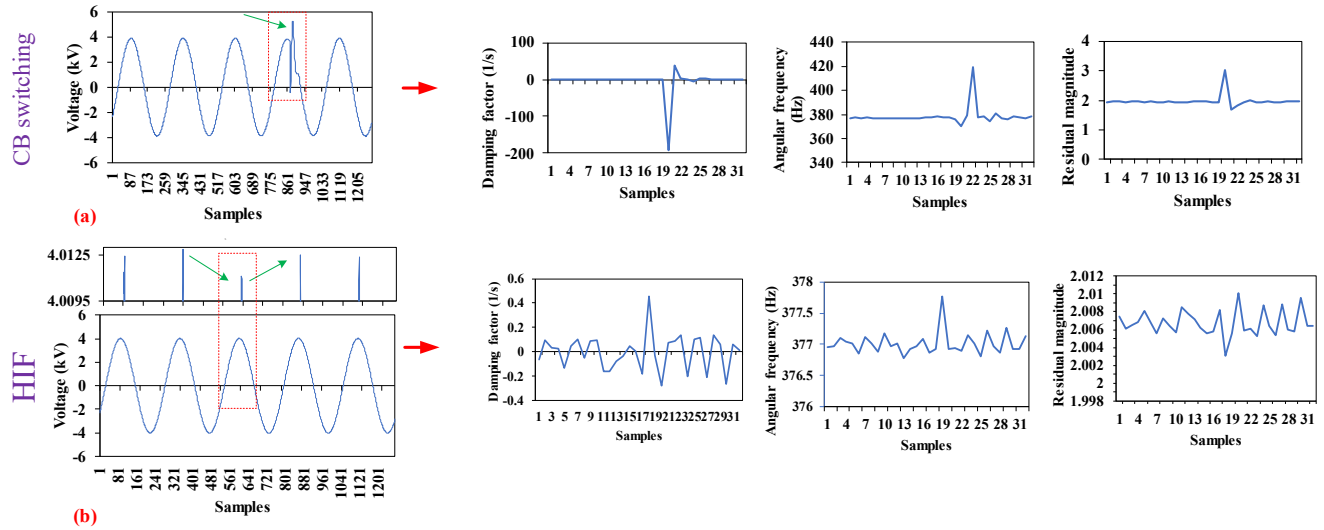


Fig. 3. Event signatures by STMPM-based feature extraction for a) CB switching and b) arcing HIF

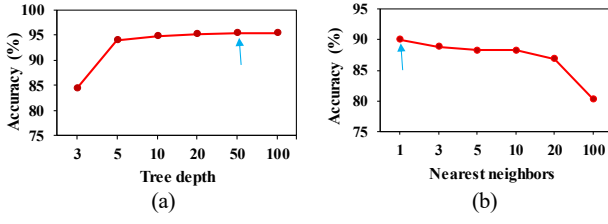


Fig. 4. The performance of base-line models, a) DT and b) kNN

sudden fluctuations, although the variations are not significant, and the measurement noise SNR is as high as 55. This analysis indicates the prominent performance of STMPM for capturing oscillatory modes of signals and its application to event classification. The proposed process is performed on all data sets and events as a pre-processing step.

#### B. Classification performance

In order to show the effectiveness of the proposed GNN-based model, two baseline models, such as decision tree (DT) and K-nearest neighbors (kNN), are considered for comparison. The data set is divided as 80-20% train-test. The performance of these methods is optimized by adjusting their parameters. In this regard, Fig. 4 illustrates that DT reaches the best accuracy under 5 different experiments by adjusting the tree depth to 50. As for the kNN, the nearest neighbor is selected to be 1. The figures in 4 show the average accuracy of 5 independent experiments. The results of the proposed grid-aware GNN method are compared with these methods which are shown in Table II. The event classification accuracy of the proposed GNN is 3.49 % and 8.24 % higher than DT and kNN. Also, GNN performs better in terms of other classification metrics. More specifically, the GNN performance is shown as a confusion matrix, indicating the classification performance

for each class, shown in Fig. 5. All classes are predicated with 100 % accuracy, but the normal operation is misclassified for 11.32 % of the time confused as a HIF event. This is because the noises on the waveform and small distortion caused by HIFs are hardly distinguishable, resulting in this confusion.

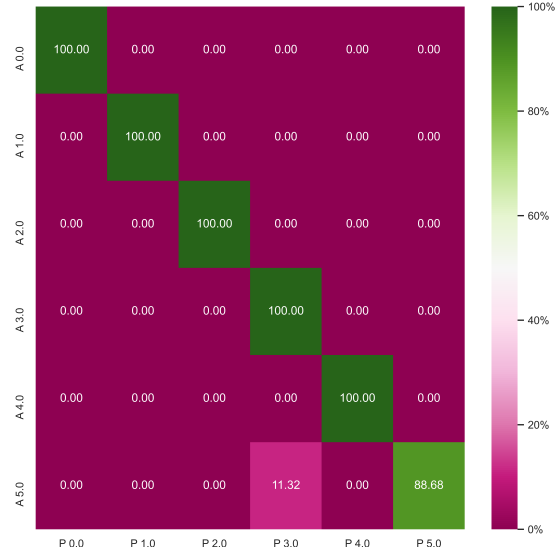


Fig. 5. The obtained confusion matrix for one of the experiments in GNN (A: Actual label, P: Predicted label)

## VI. CONCLUSIONS

In this paper, a grid-aware graph neural network (GNN) combined with short-time matrix pencil method (STMPM) analysis has been proposed, named grid-aware waveform analytics, to classify events in distribution systems. Transient load or capacitor bank switching, permanent distributed energy resource outages, low impedance, and high-impedance

faults were considered as potential events. The synchronized waveform measurement units (SWMUs) were used to capture voltage and current waveform on limited nodes, and the features were extracted using the STMPM method. The extracted features on the limited nodes along with the physical connectivity of the system were used as the input of the GNN with two layers of graph convolution to capture the spatial characteristics of events on a grid. The effectiveness of the proposed event classification was verified using the modified IEEE 13-bus system, and the results were compared with other baseline methods.

Regarding future work, this study can be extended to include phase identification of HIFs in distribution feeders. Another interesting aspect that we will be exploring is the localization of the event. Additionally, a real-time digital simulator will be adopted for event analysis and to test events in real-time.

#### ACKNOWLEDGEMENT

This material is based upon work supported by the U.S. National Science Foundation under Grant ECCS-2033927.

#### REFERENCES

- [1] B. D. Russell and C. L. Benner, "Intelligent systems for improved reliability and failure diagnosis in distribution systems," *IEEE Transactions on Smart Grid*, vol. 1, no. 1, pp. 48–56, 2010.
- [2] M. Abdelmalak, H. Hosseinpour, E. Hotchkiss, and M. Ben-Idris, "Post-disaster generation dispatching for enhanced resilience: A multi-agent deep deterministic policy gradient learning approach," in *2022 North American Power Symposium (NAPS)*, 2022, pp. 1–6.
- [3] O. Gashteroodkhani, M. Majidi, and M. Etezadi-Amoli, "Fire hazard mitigation in distribution systems through high impedance fault detection," *Electric Power Systems Research*, vol. 192, p. 106928, 2021.
- [4] I. Niazazari and H. Livani, "A PMU-data-driven disruptive event classification in distribution systems," *Electric Power Systems Research*, vol. 157, pp. 251–260, 2018.
- [5] A. F. Bastos, S. Santoso, W. Freitas, and W. Xu, "Synchronwaveform measurement units and applications," in *2019 IEEE Power Energy Society General Meeting (PESGM)*, 2019, pp. 1–5.
- [6] H. Liu, S. Liu, J. Zhao, T. Bi, and X. Yu, "Dual-channel convolutional network-based fault cause identification for active distribution system using realistic waveform measurements," *IEEE Trans Smart Grid*, 2022.
- [7] S. Xiong, Y. Liu, J. Fang, J. Dai, L. Luo, and X. Jiang, "Incipient fault identification in power distribution systems via human-level concept learning," *IEEE Trans Smart Grid*, vol. 11, no. 6, pp. 5239–5248, 2020.
- [8] M. Izadi and H. Mohsenian-Rad, "Synchronous waveform measurements to locate transient events and incipient faults in power distribution networks," *IEEE Trans Smart Grid*, vol. 12, no. 5, pp. 4295–4307, 2021.
- [9] R. Rezaiesarlak and M. Manteghi, "Short-time matrix pencil method for chipless rfid detection applications," *IEEE Transactions on Antennas and Propagation*, vol. 61, no. 5, pp. 2801–2806, 2013.
- [10] M. MansourLakouraj, R. Hossain, H. Livani, and M. Ben-Idris, "Application of graph neural network for fault location in pv penetrated distribution grids," in *2021 North American Power Symposium (NAPS)*. IEEE, 2021, pp. 01–06.
- [11] M. MansourLakouraj, M. Gautam, R. Hossain, H. Livani, M. Benidris, and S. Commuri, "Event classification in active distribution grids using physics-informed graph neural network and pmu measurements," in *2022 IEEE Industry Applications Society Annual Meeting (IAS)*, 2022, pp. 1–6.
- [12] M. MansourLakouraj, M. Gautam, H. Livani, and M. Benidris, "A multi-rate sampling pmu-based event classification in active distribution grids with spectral graph neural network," *Electric Power Systems Research*, vol. 211, p. 108145, 2022.
- [13] A. Aligholian and H. Mohsenian-Rad, "Graphpmu: Event clustering via graph representation learning using locationally-scarce distribution-level fundamental and harmonic pmu measurements," *IEEE Transactions on Smart Grid*, pp. 1–1, 2022.
- [14] M. MansourLakouraj, H. Hosseinpour, H. Livani, and M. Benidris, "Waveform measurement unit-based fault location in distribution feeders via short-time matrix pencil method and graph neural network," *IEEE Transactions on Industry Applications*, pp. 1–10, 2022.
- [15] T. N. Kipf and M. Welling, "Semi-supervised classification with graph convolutional networks," *arXiv preprint arXiv:1609.02907*, 2016.
- [16] R. Jalilzadeh Hamidi, H. Livani, and R. Rezaiesarlak, "Traveling-wave detection technique using short-time matrix pencil method," *IEEE Transactions on Power Delivery*, vol. 32, no. 6, pp. 2565–2574, 2017.
- [17] T. Sarkar and O. Pereira, "Using the matrix pencil method to estimate the parameters of a sum of complex exponentials," *IEEE Antennas and Propagation Magazine*, vol. 37, no. 1, pp. 48–55, 1995.
- [18] S. Gautam and S. M. Brahma, "Detection of high impedance fault in power distribution systems using mathematical morphology," *IEEE Transactions on Power Systems*, vol. 28, no. 2, pp. 1226–1234, 2012.